THE CARDIOVASCULAR SYSTEM AS A SMART SYSTEM

M. TRINGELOVÁ

Fakulta aplikovaných věd, Katedra mechaniky,
Západočeská univerzita v Plzni,
306 14 Plzeň, Czech Republic
E-mail: mtringel@kme.zcu.cz

P. NARDINOCCHI

Dip. Ingegneria Strutturale e Geotecnica,
Università di Roma "La Sapienza",
Via Eudossiana 18, I-00184 Roma, Italy
E-mail: paola.nardinocchi@uniroma1.it

L. TERESI* and A. DI CARLO†

SMFM@DiS, Università "Roma Tre",
Via Corrado Segre 6, I-00146 Roma, Italy
**E-mail: teresi@uniroma3.it*
†*E-mail: adicarlo@mac.com*

Our work aims at modelling and simulating the growth processes that allow the cardiovascular system to adapt to the overall body development and to changing physiological (and pathological) conditions. Within the cardiovascular system, we pay particular attention to the heart and the aorta.

A healthy aortic wall succeeds in keeping a homeostatic stress level in spite of long-standing alterations in pressure or flow by triggering growth and remodelling processes that change its stress-free shape and its structure.

A normal heart grows in response to the gradually increasing haemodynamic loading exerted on myocardial fibres. Postnatal cardiac growth is a form of volume-overload hypertrophy, produced essentially by a progressive myocardial cell enlargement, with no cell proliferation involved.

In our continuum model, growth is basically conceived of as the time evolution of the stress-free configuration of the tiny fragments into which the modelled tissue may be subdivided in imagination. It is governed by a novel balance law—the balance of accretive couples—independent of, but constitutively coupled with, the standard balance of forces.

Keywords: Cardiovascular system; adaptability; growth and remodelling.

1. The Cardiovascular System and its Adaptability

The primary function of the cardiovascular system is the transport of oxygen, carbon dioxide, nutrients, waste products within the body. Since the body undergoes major changes during its life cycle, the capability of the cardiovascular system to accommodate vastly increasing body demands is a vital requirement.

The system consists primarily of the heart, which serves as the pump, the blood, which serves as the conducting medium, and the vasculature, which serves as the conduit through which the blood flows.[1] We focus on the heart and the aorta—the main artery of the body, supplying oxygenated blood to the circulatory system. In particular, we strive to model the growth process through which the aortic wall keeps a homeostatic stress level (Section 3.1) and the postnatal hypertrophy—either physiological or pathological—of the cardiac muscle (Section 3.2). Both of these processes take place on a time scale—weeks to years—which is extremely long if compared with the heartbeat time scale (see Fig. 3). Nevertheless, understanding the basic machinery of the cardiac cycle is crucial to our endeavour, since physiological adaptation and pathological developments are both triggered by the values attained during a cardiac cycle by rather gross mechanical quantities, such as blood pressure and heart volume. This is demonstrated by an overwhelming physiological and medical evidence, even though the detailed feedback mechanisms are still largely unknown.[2]

The following two subsections collect some basic information on the structural and functional properties of the heart and the aorta, respectively, as an essential preliminary to mathematical modelling. For a fairly recent overview on the biomechanics of cardiovascular development, the reader is referred to the survey paper by Taber.[3]

1.1. *Structure and function of the heart*

The heart is a smart composite structure. Atria and ventricles have a different microstructural organization; also heart valves and ventricle walls possess a different microstructure; moreover, the heart walls are comprised of three different layers, with diverse structure and function. The inner layer—*endocardium*—and the outer layer—*epicardium*—are both very thin, each being about 100 μm thick; the middle layer, called *myocardium*, constitutes the bulk of the cardiac tissue and endows it with the ability to pump blood.

1.1.1. *The myocardium*

The myocardium is composed of cardiac *myocites* and fibroblasts, surrounded by an extracellular matrix. In adults, cardiac myocites are typically 10–20 μm in diameter and 80–125 μm in length; their cytoplasm contains mainly *myofibrils* (1–2 μm in diameter). Each myofibril consists of a string of contractile units, called *sarcomeres*, each of which is about 2 μm long. Each sarcomere consists of hundreds of filamentous protein aggregates (*myofilaments*). Thick myofilaments are composed of several hundred molecules of myosin; thin myofilaments are composed of two helically interwound polymers of actin.

Cardiac myocites are active components: they contract and relax at a high frequency producing the heartbeats; on a much longer time scale, they can grow bigger (*hypertrophy*). Muscle contraction is initiated by the release of calcium ions which are sequestered in the surrounding sarcoplasmic reticulum. A smooth ratcheting action (with a speed of about 15 μm/s) results from the shortening of the sarcomere, operated by the action of the actomyosin cross-bridges that release, move forward, and reattach. The release of calcium ions is triggered by an action potential that spreads from the cell membrane. The passage of the electrical signal from cell to cell is facilitated by the fact that myocites are highly interconnected. The biochemical mechanisms that drive the long-term hypertrophy process are more intriguing and far less understood. Some coarse-grained feedback mechanisms are hypothesized in Sec. 3.2, as a first step in our modelling effort.

The passive myocardium exhibits a nonlinear, essentially incompressible

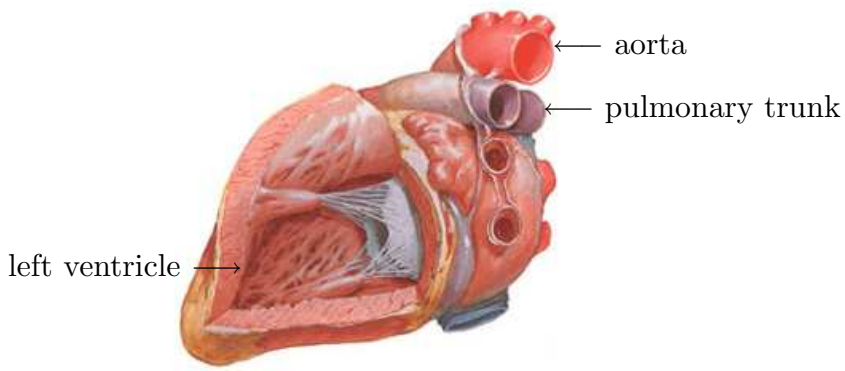

Fig. 1. View of the interior of the left ventricle, showing the mitral valve (reproduced from Ref. 4). The flap is opened in the posterolateral wall.

(visco-) elastic response, as is typical of all soft tissues. An important feature to be accounted for is the complex distribution of the predominant orientation of muscle fibres across the myocardium. In fact their orientation, while staying everywhere tangent to the wall, changes notably with position: in the equatorial region, for instance, the predominant muscle fibre direction changes from about $-65°$ in the sub-epicardial region to nearly $0°$ in the mid-wall region to about $+65°$ in the sub-endocardial region, all relative to the circumferential direction. This transmural splay of fibre directions causes the heart to twist during the cardiac cycle.[1] Another peculiar feature that cannot be disregarded is the existence of a major self-stress that contributes to a more uniform intramural stress distribution under physiological conditions. The self-stress is distributed across the heart wall in a way closely related to the fibered structure of the myocardium, as shown by a series of tests performed by Omens and Fung[5] on rat left ventricles about twenty years ago and recently reported by Humphrey.[1] Evidence of compressive circumferential residual stress in equatorial rings of myocardium tissue excised from the left ventricle was obtained by effecting radial cuts that left the rings open and stress-free. A comparison of the length of sarcomeres in this stress-free configuration with the one they had in the intact configuration showed that, while the relaxed length of sarcomeres varies significantly from the endocardium to the epicardium in the unloaded (but self-stressed) myocardium configuration, it is nearly uniform across the wall in the stress-free configuration.

1.1.2. *The cardiac cycle*

The main heart function is to ensure blood pumping into both the high pressure *systemic circuit* and the low pressure *pulmonary circuit* (see Fig. 2). The cardiac cycle may be split into four stages (see Fig. 3). The first is the *diastolic filling* (comprising phases 6,7 and 1 in Fig. 3), which is started by the opening of the valve connecting the left atrium with the left ventricle—the mitral valve. This stage is characterized by a dilation of the left ventricle caused by the higher pressure in the atrium and progressively slowed down by the increasing apparent stiffness of the ventricle wall. During the diastolic filling, the pressure in the left ventricle does not change significantly, achieving a maximum of 15 mmHg (= 2 KPa), versus an aortic pressure of 90 mmHg. The contraction of myocardial fibres makes the mitral valve close, thus starting the second stage of the cardiac cycle—the *isovolumic contraction* (phase 2 in Fig. 3). The left-ventricle pressure rises rapidly dur-

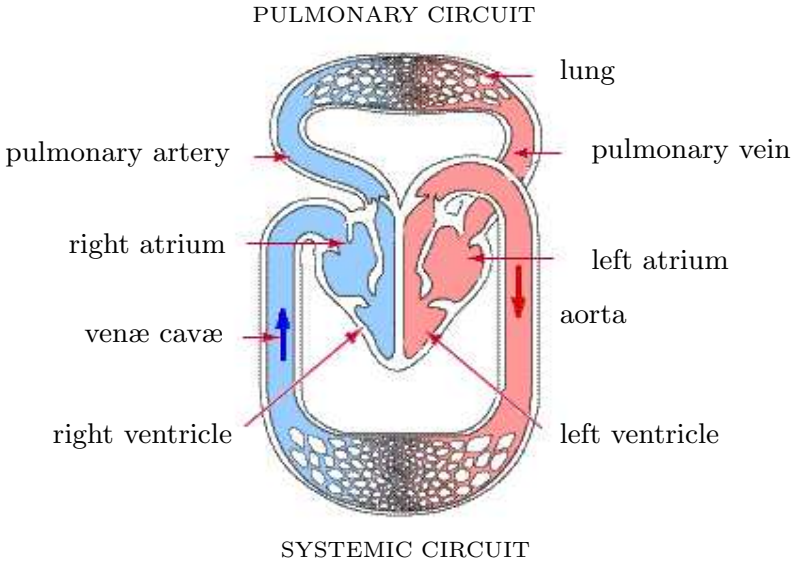

Fig. 2. A heart-centred schematic picture of blood circulation (reproduced from Ref. 6): the upper part schematizes the pulmonary circuit, the lower part the systemic circuit; the left side carries oxygen-poor blood, the right side oxygen-rich blood.

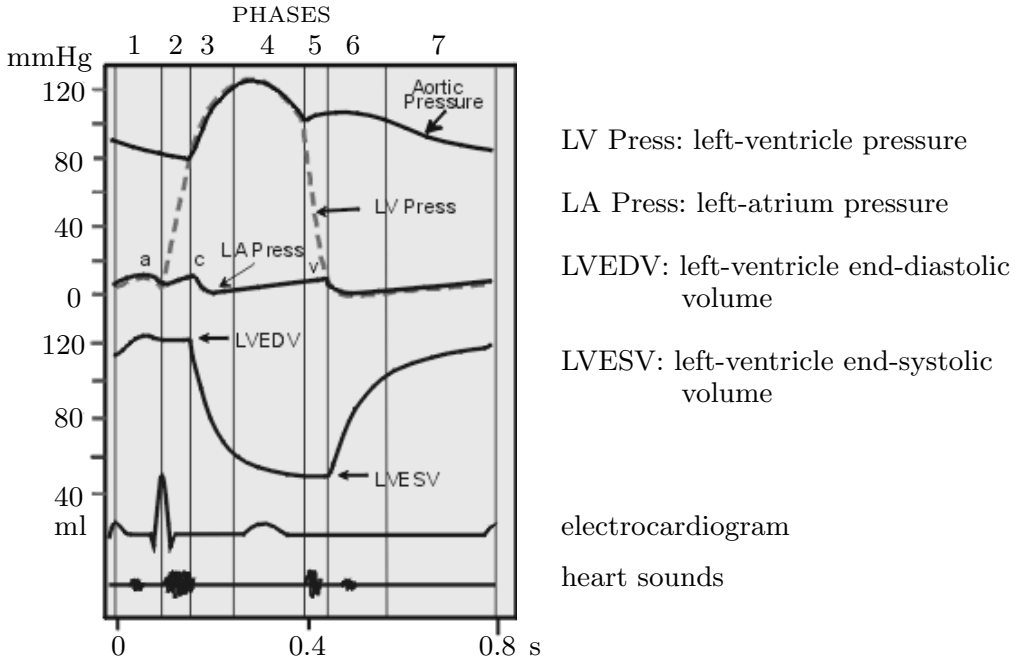

Fig. 3. Pressure and volume monitored along a cardiac cycle (reproduced from Ref. 7)

ing this stage, and the aortic valve opens when it exceeds the aortic pressure. On the contrary, the volume of the left ventricle does not change, as it stays filled with blood. The stage of *systolic ejection* (comprising phases 3 and 4 in Fig. 3) starts with the opening of the aortic valve. Most of the cardiac output is provided in the first quarter of this stage, before the pressure peaks at about 120 mmHg. Then, when the pressure drops to about 100 mmHg, the aortic valve closes, starting the fourth stage: the *isovolumic relaxation* (phase 5 in Fig. 3). During this stage the volume of the left ventricle keeps its minimum value, while the left ventricular pressure drops fast to the value of the atrial pressure, triggering the opening of the mitral valve and starting a new cardiac cycle.

1.2. *The aorta as a prototype large vessel*

Arteries are roughly classified as *elastic* or *muscular*. Elastic arteries are larger and are located close to the heart, like the aorta; muscular arteries are smaller and closer to the arterioles. The walls of both elastic and muscular arteries consist of three different layers: *intima*, *media*, and *adventitia*.

The intima, which is the innermost of the threes and consists of a single layer of endothelial cells, is extremely thin with respect to the arterial wall, at least in large arteries. Its contribution to the mechanical properties of the wall may only become significant in old age or under degenerative conditions: atherosclerosis, in fact, implies a thicker and stiffer intima. The middle layer—the media—is characterized by a complex mixture of smooth muscle cells, elastin and collagen fibrils. Vascular smooth muscles modify the distensibility of large arteries and regulate the lumen size in medium and small arteries. Consistent with their different roles, smooth muscles are organized differently in large (elastic) and in small (muscular) arteries. In elastic arteries, vascular smooth muscles are organized in musculoelastic fascicles—that is, alternate layers of smooth muscle and elastin (up to 70 layers in the human aorta). In muscular arteries, elastin is absent and smooth muscles form a single layer embedded in a matrix of connective tissue. The outermost layer—the adventitia—consists primarily of collagen fibres arranged in helical structures. It contributes significantly to the strength of the arterial wall.

The mechanical properties of an arterial wall are approximately homogeneous within each single layer, but not overall. In fact, the difference in stiffness exhibited by different layers plays an important role in the adaptive response of the arterial wall to perturbations from its homeostatic state. The differential growth of the layers originates a non uniform self-stress dis-

tribution within the wall. Such self-stress (also called residual stress) has been extensively investigated, due to its importance in stress redistribution and vascular remodelling. When excised from the vascular tree, an arterial segment shortens drastically. A further radial cut releases most of the residual stress in an unloaded intact arterial ring, allowing it to open up, the opening angle being a rough measurable indicator of the preexisting self-stress (see Refs. 8, 9 and our discussion in Sec. 3.1).

The aorta, like the other large arteries, exhibits a highly nonlinear behaviour under large strains. A constitutive model of such behaviour should account for both its passive response, due to elastin and collagen, and its active response, due to muscle fibres. Following the fluctuations of the intramural pressure, the arterial wall undergoes instantaneous elastic deformations, essentially determined by its passive response. Despite its complexities, such a response is by no means the most characteristic mechanical property of the arterial wall as a living tissue. When the normal conditions are altered for a sufficiently long time, the passive response may be supplemented by a suitable contraction of the vascular smooth muscles, that constitutes the primary adaptive mechanism aiming at keeping the flow-induced shear stress and the wall stress distribution at their baseline values. Of course, such a goal is achieved at the expense of an altered contractile state of smooth muscle cells.[10,11] Therefore, alterations in pressure or flow which hold out over long periods of time (days, weeks) trigger a different adaptive response, consisting in growth and remodelling processes that modify the stress-free shape and the structure of the vessel wall.

The passive mechanical response of arterial walls has been extensively investigated through uniaxial, biaxial, and torsion tests. On the contrary, very few data are available on the active response of vascular smooth muscles. Moreover, these data come only from uniaxial tests performed on arterial rings or helical strips excised from an artery following the local orientation of the muscle fibres. Therefore, they cannot account for the effects of the complex three-dimensional arrangement of these fibres. Even less is known of the long-term adaptive response implying growth and remodelling.

2. Gross Mechanics of Bulk Growth

We concentrate on the growth phenomena which are key to the adaptability of the cardiovascular system—and, more generally, of all smart living systems. In Section 3 we offer the results of our preliminary simulations of the adaptive remodelling of arterial walls (Section 3.1) and sketch the conceptual underpinning of our incipient project aiming at modelling post-

natal cardiac hypertrophy (Section 3.2). The present section is devoted to a condensed, but reasonably self-contained, presentation of the theoretical framework common to both models, based on the dynamical theory of growth introduced by DiCarlo and Quiligotti.[12] We follow the lines of Ref. 13, where an abridged account of the theory of bulk growth was given as a preliminary to the treatment of surface growth.[a] A comprehensive account of experimental and theoretical issues in the biomechanics of growth and remodelling may be found in the review papers by Taber[15] and Cowin.[16]

2.1. *Kinematics: gross and refined motions*

We regard a growing piece of tissue—which we call the *body* in the rest of Sec. 2—as a smooth manifold $\mathscr{B}$ (with boundary $\partial\mathscr{B}$), and call (*gross*) *placement* any smooth embedding

$$p : \mathscr{B} \to \mathscr{E} \tag{1}$$

of the body into the Euclidean *place manifold* $\mathscr{E}$, whose translation space will be denoted by $\mathrm{V}\mathscr{E}$. Tangent vectors on the body manifold itself are called *line elements*. The set of all line elements attached to a single body-point $b \in \mathscr{B}$ is called the *body element* at b, and denoted $\mathrm{T}_b\mathscr{B}$ (the tangent space to $\mathscr{B}$ at b). The union of all body elements is denoted $\mathrm{T}\mathscr{B}$ (the tangent bundle of $\mathscr{B}$).

The *body gradient* ∇p of a placement p is a tensor field on $\mathscr{B}$, whose value at any given point b, denoted by $\nabla p|_b$, maps linearly the body element $\mathrm{T}_b\mathscr{B}$ onto $\mathrm{V}\mathscr{E}$. We call *element-wise configuration*—or, with a much shorter monosyllable, *stance*—any tensor field of this kind, be it a gradient or not. Therefore, a stance is any smooth mapping

$$\mathrm{P} : \mathrm{T}\mathscr{B} \to \mathrm{V}\mathscr{E}, \tag{2}$$

such that the restriction $\mathrm{P}|\mathrm{T}_b\mathscr{B}$ is a linear embedding, for all $b \in \mathscr{B}$. If a stance happens to be the gradient of a placement, we say that it is induced by that placement: all placement induces a stance, but a general stance is not induced by any placement, not even locally.

In order to distinguish growth from passive deformation, we postulate that, at each time $\tau \in \mathscr{T}$ (the *time line*, identified with the real line), there exists a dynamically distinguished stance $\mathbb{P}(\tau)$—smoothly depending

[a] The same theory encompasses also modes of material remodelling that are not treated here nor in Refs. 12, 13, such as the evolution of the elastic stiffness due to microstructural rearrangements: see Ref. 14 for a treatment of the remodelling of anisotropic bone tissue.

on time—which we call *prototypal stance* or, briefly, *prototype*. The assignment of a gross placement and a prototype to each time defines a *refined motion* $(p, \mathbb{P})$. The idea to refine the gross motion in this way dates back to Kröner[17] and Lee,[18] who introduced the notion of an "intermediate" configuration in the sixties, to distinguish between elastic and visco-plastic strains. Much later Rodriguez, Hoger and McCulloch imported that notion into biomechanics, reinterpreting it as the "zero-stress reference state" of a growing body element, to quote verbatim from their 1994 paper.[19]

The velocity *realized* along the refined motion $(p, \mathbb{P})$ at the time $\tau \in \mathscr{T}$ is the pair of fields (a superposed dot denoting time differentiation):

$$(\,\dot{p}(\tau), \dot{\mathbb{P}}(\tau)\mathbb{P}(\tau)^{-1}) : \mathscr{B} \to \mathrm{V}\mathscr{E} \times (\mathrm{V}\mathscr{E} \otimes \mathrm{V}\mathscr{E})\,. \tag{3}$$

The linear space of *test velocities* $\mathfrak{T}$, comprising all smooth fields

$$(\mathrm{v}, \mathbb{V}\,) : \mathscr{B} \to \mathrm{V}\mathscr{E} \times (\mathrm{V}\mathscr{E} \otimes \mathrm{V}\mathscr{E})\,, \tag{4}$$

will play a central role in Sec. 2.2. The *gross velocity* of body-points is given by the vector field v, while the tensor field $\mathbb{V}$ gives the *growth velocity* of the corresponding body elements.

2.2. *Dynamics: brute and accretive forces; balance principle*

A *force* is primarily a continuous[b] linear real-valued functional on the space of test velocities, whose value we call the *working* expended by that force. We assume that the *total* working—*i.e.*, the working expended by the sum of all forces at play—expended on any test velocity $(\mathrm{v}, \mathbb{V}\,) \in \mathfrak{T}$ admits the following integral representation:

$$\int_{\mathscr{B}} \big(\,\mathbb{A}^{\mathrm{i}} \cdot \mathbb{V} - \mathrm{S} \cdot \mathrm{Dv}\,\big) \;+ \int_{\mathscr{B}} (\,\mathrm{b} \cdot \mathrm{v} + \mathbb{A}^{\mathrm{o}} \cdot \mathbb{V}\,) \;+ \int_{\partial\mathscr{B}} \mathrm{t}_{\partial\mathscr{B}} \cdot \mathrm{v}\,, \tag{5}$$

where the integrals are taken with respect to the bulk volume and surface area of body elements in their prototypal configuration—to be called *prototypal volume* and *prototypal area*, for short—, and

$$\mathrm{Dv} := (\nabla \mathrm{v})\mathbb{P}^{-1} \tag{6}$$

denotes the *prototypal gradient* of v (shorthand for 'Euclidean representation of the body gradient ∇v mediated by the prototypal configuration').

[b] Continuity of force functionals is physically essential; to make it meaningful, the space of test velocities should be endowed with the structure of a *topological* vector space. We gloss over this issue, leaving up to the mathematically conscious reader the task to complete the space of smooth test fields $\mathfrak{T}$ in a topology appropriate to Eq. (5).

Because of the compound structure of test velocities, the force functional splits additively into a *brute force*, dual to v, and an *accretive force*, dual to $\mathbb{V}$. Another important splitting—to be discussed in Sec. 2.4—is between the *inner* working, given by the first bulk integral in Eq. (5), and the *outer* working, given by the remaining sum. The *brute bulk-force* per unit volume b and the *brute boundary-force* per unit area $\mathrm{t}_{\partial\mathscr{B}}$ take values in $\mathrm{V}\mathscr{E}$; the *inner* (*outer*) *accretive couple* per unit volume $\mathbb{A}^{\mathrm{i}}$ ($\mathbb{A}^{\mathrm{o}}$) and the *brute Piola stress* S—also a specific couple—take values in $\mathrm{V}\mathscr{E}\otimes\mathrm{V}\mathscr{E}$.

All balance laws are systematically provided by the universal *balance principle* stating that, at each time, the total working expended on any test velocity should be zero, *i.e.*, all forces at play should sum up to the null functional. Via standard localization arguments, this yields the local statements of balance:

$$\textit{balance of brute forces:}\ \operatorname{Div}\mathrm{S}+\mathrm{b}=0\ \text{ on }\mathscr{B}\ \ \&\ \ \mathrm{S}\,\mathrm{n}_{\partial\mathscr{B}}=\mathrm{t}_{\partial\mathscr{B}}\ \text{ on }\partial\mathscr{B}\,; \tag{7}$$

$$\textit{balance of accretive couples:}\ \mathbb{A}^{\mathrm{i}}+\mathbb{A}^{\mathrm{o}}=0\ \text{ on }\mathscr{B}. \tag{8}$$

In Eq. (7), $\operatorname{Div}\mathrm{S}$ is the only vector field satisfying the scalar identity

$$\operatorname{div}(\mathrm{S}^{\top}\mathrm{v})=(\operatorname{Div}\mathrm{S})\cdot\mathrm{v}+\mathrm{S}\cdot\mathrm{Dv}$$

for each vector field v, while the divergence of a vector field is the trace of its prototypal gradient: $\operatorname{div}\mathrm{v}=(\mathrm{Dv})\cdot\mathrm{I}$, I being the identity on $\mathrm{V}\mathscr{E}$; $\mathrm{n}_{\partial\mathscr{B}}$ is the outward unit normal to the facets in $\partial\mathscr{B}$ in their prototypal configuration. Once brute forces and accretive couples are constitutively related to the refined motion, the balance principle rules out all refined motions that do not satisfy Eqs. 7 and 8 at all times.

2.3. *Energetics*

To parametrize the state of the body, an additional energetic descriptor is needed. We postulate the existence of a real-valued *free energy* measure, such that the energy available to any part $\mathscr{P}$ of $\mathscr{B}$ is given by $\Psi(\mathscr{P})=\int_{\mathscr{P}}\psi$, where the density ψ is the free energy per unit prototypal volume (the integral being taken with respect to the bulk volume of body elements in their prototypal configuration). A body-part is a body-like subset of $\mathscr{B}$.

2.4. *Constitutive issues: theory and recipes*

The constitutive theory of inner forces rests on two main pillars, altogether independent of balance: the principle of material indifference to change in observer, and the dissipation principle. Both of them deliver strict selection

rules on admissible constitutive recipes for the inner force. None of them applies to the outer force, which has to be regarded as an adjustable control on the motion. In fact, while the inner force represents the interactions among the (few) degrees of freedom resolved by the theory, the outer force represents their interactions with the (myriad) degrees of freedom in the universe whose evolution is not described by the motion—however refined. Not all the degrees of freedom left unresolved by the theory are necessarily localized outside of the body it considers, since its resolution is limited not only in breadth, but also—and possibly more importantly—in depth. Therefore, the crucial inner/outer dichotomy encompasses, but does not coincide with, the more obvious distinction internal/external to the body. A force is inner or outer with respect to the theory, not to the body: what appears as an outer force within a given theory may always—in principle— be accounted for as inner within a broader, deeper and more cumbersome theory. In an all-embracing theory there would be no outer force at all. In our theory of the biomechanics of growth, the outer accretive couple $\mathbb{A}^{\mathrm{o}}$ plays a primary role, representing the mechanical effects of the biochemical control system, smartly distributed within the body itself: ignoring the chemical degrees of freedom does not make negligible their feedback on mechanics.

2.4.1. *Material indifference to change in observer*

The group $\mathfrak{O}$ of changes in observer we consider consists of all smooth maps of the time line $\mathscr{T}$ into the group of isometries of $\mathscr{E}$, $\mathrm{Isom} \simeq \mathscr{O} \times \mathrm{V}\mathscr{E}$, $\mathscr{O}$ being the group of orthogonal transformations of $\mathrm{V}\mathscr{E}$. Taking for granted the action of $\mathfrak{O}$ on the set of gross motions, we extend it to the set $\mathfrak{P}$ of refined motions as follows: a change in observer $(\widetilde{\mathrm{Q}}, \widetilde{\mathrm{u}}) \in \mathfrak{O}$ transforms $(p, \mathbb{P}) \in \mathfrak{P}$ into the *corresponding* refined motion $(\widetilde{p}, \widetilde{\mathbb{P}})$, defined by

$$\widetilde{p}(b,\tau) = \widetilde{x}_{\mathrm{o}}(\tau) + \widetilde{\mathrm{Q}}(\tau)\,(\,p\,(b,\tau) - x_{\mathrm{o}}(\tau))\,, \qquad \widetilde{\mathbb{P}}(b,\tau) = \mathbb{P}(b,\tau)\,, \tag{9}$$

for each $b \in \mathscr{B}$, $\tau \in \mathscr{T}$. In Eq. (9), $x_{\mathrm{o}}(\tau) \in \mathscr{E}$ is the centre of the spherical isometry $(\widetilde{\mathrm{Q}}(\tau), 0)$, and $\widetilde{x}_{\mathrm{o}}(\tau) := x_{\mathrm{o}}(\tau) + \widetilde{\mathrm{u}}\,(\tau)$. Notice that $\mathfrak{O}$ acts trivially on prototypal stances: this trivial extension, while strongly motivated, is by no means obvious and has momentous consequences.[c] Consequently, the velocity $(\widetilde{\mathrm{v}}, \widetilde{\mathbb{V}}\,)$ corresponding to $(\mathrm{v}, \mathbb{V}\,)$ is

$$\widetilde{\mathrm{v}}(b) = \widetilde{\mathrm{Q}}(\tau)\,\mathrm{v}(b) + \widetilde{\mathrm{w}}(\tau) + \widetilde{\mathrm{W}}(\tau)\,(\,\widetilde{p}\,(b,\tau) - \widetilde{x}_{\mathrm{o}}(\tau))\,, \qquad \widetilde{\mathbb{V}}(b) = \mathbb{V}(b)\,, \tag{10}$$

with $\widetilde{\mathrm{w}}(\tau) := \dot{\widetilde{x}}_{\mathrm{o}}(\tau) - \widetilde{\mathrm{Q}}(\tau)\,\dot{x}_{\mathrm{o}}(\tau)$, and $\widetilde{\mathrm{W}}(\tau) := \dot{\widetilde{\mathrm{Q}}}(\tau)\,\widetilde{\mathrm{Q}}(\tau)^{\top}$.

[c] For the crippling consequences of a different, nontrivial extension, see Ref. 20.

The *principle of material indifference to change in observer* requires that, under an arbitrary change in observer $(\widetilde{\mathrm{Q}}, \widetilde{\mathrm{u}}) \in \mathfrak{O}$, the working expended over each body-part on each test velocity $(\mathrm{v}, \mathbb{V})$ by the inner force constitutively related to each refined motion $(p, \mathbb{P})$ at any given time should be equal to the working expended on the corresponding velocity $(\widetilde{\mathrm{v}}, \widetilde{\mathbb{V}})$ (at the same time, over the same body-part) by the inner force related by the same constitutive prescription to the corresponding refined motion $(\widetilde{p}, \widetilde{\mathbb{P}})$. A parallel requirement of the same principle is that the free energy Ψ should be constitutively prescribed in such a way as to be invariant under all change in observer. Since arbitrarily small parts can be taken around any body-point, these identities localize at each body-point $b \in \mathscr{B}$.

The above principle rules out non-symmetric values of the *brute Cauchy stress* $\mathrm{T} := (\det \mathrm{F})^{-1}\, \mathrm{S}\, \mathrm{F}^{\top}$, where the *warp*

$$\mathrm{F} := \mathrm{D}p = (\nabla p)\, \mathbb{P}^{-1} \tag{11}$$

measures how the gross stance, *i.e.*, the body gradient of the gross placement, differs from the prototypal stance. If we further assume that the response of the body element at b filters off from $(p, \mathbb{P})$ all information other than $p|_b$, $\nabla p|_b$, and $\mathbb{P}|_b$, we obtain the following *reduction theorem*: there are constitutive mappings $\widehat{\mathrm{S}}_b$, $\widehat{\mathbb{A}}^{\mathrm{i}}_b$ and $\widehat{\psi}_b$ such that

$$\mathrm{S}(b,\tau) = \mathrm{R}(b,\tau)\, \widehat{\mathrm{S}}_b(\ell_b, \tau), \quad \mathbb{A}^{\mathrm{i}}(b,\tau) = \widehat{\mathbb{A}}^{\mathrm{i}}_b(\ell_b, \tau), \quad \psi(b,\tau) = \widehat{\psi}_b(\ell_b, \tau), \tag{12}$$

where the constitutive list ℓ_b reduces to

$$\ell_b := (\, \mathrm{U}|_b, \mathbb{P}|_b\,), \tag{13}$$

the *rotation* R and the *stretch* U being, respectively, the orthogonal and the right positive-symmetric factor of the warp: $\mathrm{F} = \mathrm{R}\,\mathrm{U}$.

2.4.2. *Dissipation principle*

We call *power expended* along a refined motion at any given time the opposite of the working expended by the inner force constitutively related to that motion on the velocity realized along the motion at the given time. Hence, the power expended measures the working done by a putative outer force balanced with the constitutively determined inner force. The *dissipation principle* we enforce requires that the *power dissipated*—defined as the difference between the power expended along a refined motion and the time derivative of the free energy along that motion—should be non-negative, for all body-parts, at all times. This localizes into:

$$\dot{\psi} + \psi\, \mathrm{I} \cdot (\, \dot{\mathbb{P}}\mathbb{P}^{-1}) \;\leq\; \mathrm{S} \cdot (\mathrm{D}\,\dot{p}) \;-\; \mathbb{A}^{\mathrm{i}} \cdot (\, \dot{\mathbb{P}}\mathbb{P}^{-1}), \tag{14}$$

it being intended that S, $\mathbb{A}^{\mathrm{i}}$ and ψ are given by Eq. (12). The second term on the left side of Eq. (14) stems from the fact that the prototypal-volume form, say ω, evolves in time as dictated by the growth velocity $\dot{\mathbb{P}}\mathbb{P}^{-1}$:

$$\dot{\Psi}(\mathscr{P}) = \left(\int_{\mathscr{P}} \psi\,\omega\right)^{\cdot} = \int_{\mathscr{P}} (\psi\,\omega)^{\cdot} = \int_{\mathscr{P}} (\dot{\psi}\,\omega + \psi\,\dot{\omega}) = \int_{\mathscr{P}} \left(\dot{\psi} + \psi\,\mathrm{I}\cdot(\dot{\mathbb{P}}\mathbb{P}^{-1})\right)\omega.$$

2.4.3. *Constitutive assumptions: free energy and inner force*

Our main constitutive assumption concerns the free energy. We posit that, for each body-point b at any given time τ, $\psi(b,\tau)$ depends solely on the value $\mathrm{F}(b,\tau)$ of the warp at that time (in fact, only on the value $\mathrm{U}(b,\tau)$ of the stretch, because of Eqs. 12, 13): there exists a map φ_b such that[d]

$$\psi(b,\tau) = \widehat{\psi}_b(\,\mathrm{U}|_b, \mathbb{P}|_b, \tau) = \varphi_b\,(\mathrm{F}(b,\tau))\,. \tag{15}$$

The requirement that Eq. (14) be satisfied along all refined motions is fulfilled if and only if for each b (which will be dropped from now on) the mappings $\widehat{\mathrm{S}}$ and $\widehat{\mathbb{A}}^{\mathrm{i}}$ satisfy:

$$\widehat{\mathrm{S}} = \partial\varphi + \overset{+}{\mathrm{S}}\,, \qquad \widehat{\mathbb{A}}^{\mathrm{i}} = \mathbb{E} + \overset{+}{\mathbb{A}}\,, \tag{16}$$

where ∂ denotes differentiation. The *Eshelby couple*

$$\mathbb{E} := \mathrm{F}^{\top}\,\widehat{\mathrm{S}} - \varphi\,\mathrm{I} \tag{17}$$

bridges between brute and accretive mechanics; the *extra-energetic* responses $\overset{+}{\mathrm{S}}$, $\overset{+}{\mathbb{A}}$ are restricted by the *reduced dissipation inequality*

$$\overset{+}{\mathbb{A}}(\ell,\tau)\cdot(\,\dot{\mathbb{P}}(\tau)\mathbb{P}(\tau)^{-1}) - \overset{+}{\mathrm{S}}(\ell,\tau)\cdot\dot{\mathrm{F}}(\tau) \;\leq\; 0\,, \tag{18}$$

to be abided by along all refined motions, at all times (ℓ being given by Eq. (13)). We regard all dissipative mechanisms extraneous to growth to be negligible, assuming the extra-energetic brute stress to be null: $\overset{+}{\mathrm{S}}=0$. Then, we make Eq. (18) satisfied in the most facile—though scarcely warranted—way, letting the extra-energetic accretive couple be simply proportional to the growth velocity through a prescribed negative scalar factor:

$$\overset{+}{\mathbb{A}}(\ell\,,\tau) = -c\,\dot{\mathbb{P}}(\tau)\mathbb{P}(\tau)^{-1}, \tag{19}$$

the *resistance to growth* c being positive: $c>0$.

In our preliminary simulations, we specify the free-energy map φ thinking of a putatively homogenized material, in order to avoid detailing the

[d] See the paper[21] by Epstein for an insightful discussion of the implications of Eq. (15).

micro-geometry, a common practice in similar applications.[23–26] In particular, following Humphrey and Yin,[23,24] we envisage to model the passive myocardium response assuming that φ splits additively into an isotropic component φ^{m}, accounting for the matrix surrounding the fibres, and a transversely isotropic component φ^{f}, accounting for the oriented collagen fibres: $\varphi = \varphi^{\mathsf{m}} + \varphi^{\mathsf{f}}$. Our first results on growth-induced self-stress in arteries, summarized in Sec. 3.1, have been obtained in the most simplistic way, disregarding anisotropy altogether: $\varphi^{\mathsf{f}} = 0$, and identifying the isotropic component as *neo-Hookean*:

$$\varphi(\mathrm{F}) = \varphi^{\mathsf{m}}(\mathrm{F}) = \tfrac{1}{2}\,\mu\,\big(\mathrm{F}\cdot\mathrm{F} - 3\big)\,, \tag{20}$$

where the single scalar parameter $\mu > 0$ is a shear modulus; Eq. (20) has to be complemented by the incompressibility constraint: $\det \mathrm{F} = 1$.

2.4.4. *Constitutive assumptions: outer force*

In the intended applications, the brute bulk-force plays a negligible role: we assume $\mathrm{b} = 0$. The brute boundary-force $\mathrm{t}_{\partial\mathscr{B}}$ represents blood pressure and contact interactions with surrounding tissues. The key assumption is the one concerning the outer accretive couple $\mathbb{A}^{\mathsf{o}}$, whose constitutive prescription should hopefully short-circuit the complex—and ill-understood—sensing/actuating mechanobiological functions that control growth.

We offer a preliminary, crude recipe we have being using for simulating the adaptive remodelling of arterial walls (see Sec. 3.1 and Ref. 22); the contrivance of an analogous recipe for postnatal cardiac hypertrophy is still in progress (see Sec. 3.2). Inspired by the stress-dependent growth laws proposed by Taber,[27–29] we posit a *target Cauchy stress* $\mathrm{T}^{\odot}$ (as detailed in Sec. 3.1) and assume

$$\mathbb{A}^{\mathsf{o}} = \varphi\,\mathrm{I} - (\det \mathrm{F})\,\mathrm{F}^{\top}\mathrm{T}^{\odot}\,\mathrm{F}^{-\top}, \tag{21}$$

in order that the outer accretive couple compensates for the Eshelby couple if and only if the target stress is met:

$$\mathbb{E} + \mathbb{A}^{\mathsf{o}} = \mathrm{F}^{\top}(\,\mathrm{T} - \mathrm{T}^{\odot})\,\mathrm{F}^{-\top}. \tag{22}$$

3. Mathematical Models of Adaptive Growth

3.1. *Growth-induced residual stress in large arteries*

As mentioned in Sec. 1.2, the fact that in vivo arteries are highly self-stressed is revealed by two salient phenomena. Soon after an arterial segment is excised and removed, its undergoes a conspicuous longitudinal

shortening, the ratio between the in vivo and excised lengths ranging from 1.4 to 1.7. Furthermore, when a shallow ring-shaped segment is cut in the radial direction, the ring springs open into a sector (see Fig. 4c). A coarse evaluation of the preexisting residual stress is obtained by measuring the opening angle, defined as the angle subtended by two segments drawn from the midpoint of the inner wall to the tips of the open section. The opening angle varies widely with the organ in which the blood vessel is located, with its size and shape, and with tissue remodelling. The opening angle is larger where the vessel is more curved, or thicker. For example, the opening angle

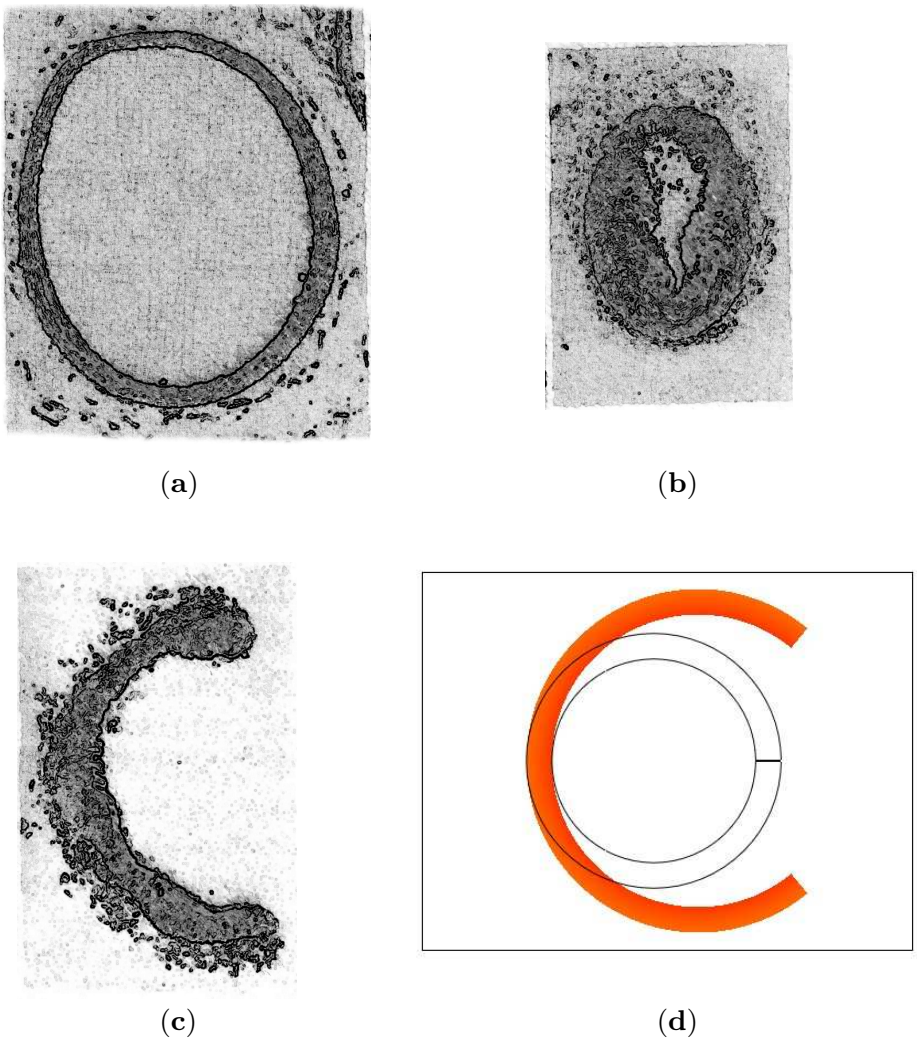

Fig. 4. Photographs reproduced from Ref. 8: (a) cross section of a rat pulmonary artery fixed in vivo at normal pressure; (b) after excision; (c) after stress release. Our simulation (see text): (d) opening angle for a rat aorta = 58°.

of a normal rat artery is about 160° in the ascending aorta, 90° in the arch, 60° in the thoracic region, 80° in the abdomen.[8]

We try to relate the opening angle measured *ex vivo* with the growth experienced *in vivo* by solving numerically the evolution equation

$$\dot{\mathbb{P}} = c^{-1}\Big(\mathrm{F}^{\top}(\mathrm{T} - \mathrm{T}^{\odot})\, \mathrm{F}^{-\top}\Big)\, \mathbb{P} \tag{23}$$

deriving from Eqs. (8), (12), (16), (17), (19), (22), coupled with the standard equation for nonlinear elasticity deriving from Eqs. (7), (11), (12), (15), (16), (20). This is done on a 2D computational domain, the annular cross section of a cylindrical vessel mimicking a rat aorta: lumen radius = 0.2 mm, wall thickness = 50 μm (data taken from Ref. 27), shear modulus $\mu = 170$ KPa. We assume this configuration to be initially stress-free and solve a cascade of four problems: (i) passive response under intramural pressure = 16 KPa and longitudinal stretch = 1.6; (ii) active response (2D growth) obtained by integrating Eq. (23) from the solution to problem (i) to a steady state, $\mathrm{T}^{\odot}$ being pinpointed by two criteria: (1) to have a constant hoop component, and (2) to satisfy Eq. (7); (iii) passive response under removal of pressure and longitudinal tension (simulated excision) from the steady state reached in (ii); (iv) same as in (iii) for the cut annulus (see Fig. 4d).

3.2. *Towards a gross mechanics of cardiac hypertrophy*

To attack the complex problem of modelling the growth of the human heart from infancy to adulthood, we concentrate first on its most important component, the left ventricle. Three months after birth, cardiac myocites stop proliferating; however, they get longer and wider by synthesizing more proteins. This slow process, that develops in response to the increasing haemodynamic loading due to the overall body development and to physical exercise,[30] is a form of volume-overload hypertrophy.[31] It is absolutely physiological, even though it admits dangerous, possibly lethal, pathological variants.

The basic tenet of our model is that cardiac hypertrophy is chiefly driven by brute mechanical circumstances associated with the myocardial pump function, with other factors playing a minor role. As a secondary, provisional hypothesis, we admit that the hypertrophic process can be described—at least to a first approximation—by the sole evolution of the stress-free geometry of the cardiac tissue, without any modification of its microstructure and functionality.[e] Within the cardiac cycle (see Fig. 3), two events are

[e]Seemingly, this hypothesis has to be removed to cover pathological forms of hypertrophy.

critical in determining the pumping efficiency of the left ventricle: the closure of the mitral valve (separating phase 1 from 2: notice the spike in the electrocardiogram), and the opening of the aortic valve (separating phase 2 from 3: the left-ventricle pressure crosses over the aortic pressure).

The closure of the mitral valve at the end of the diastolic filling and the successive systolic ejection are operated by the isometric contraction of myocardial fibres. Now, the optimum overlapping between actin and myosin filaments in sarcomeres is obtained when the sarcomere length lies between 1.8 and 2.2 μm: if the sarcomeres were longer (or shorter), the force exerted by the contraction of myocardial fibres would be smaller. Taking it for granted that the ventricle size has to increase with age and physical exercise to accommodate a larger blood volume, the only way to keep the sarcomeres at their optimal relaxed length is to multiply their number by synthesizing longer myofibrils within the preexisting cardiac myocites—whose number does not increase, as already noted.

In order for the aortic valve to open, it is necessary that the left-ventricle pressure exceeds the aortic pressure. Now, the value attained by the pressure inside the ventricle at the end of the isovolumic contraction is directly correlated with the stress generated within the ventricle wall by the myocardial contraction.[32] A crude estimate of this correlation is readily provided by a simplistic application of Laplace's formula for a pressurized thin-walled spherical container, establishing that the ratio (surface tension)/(intramural pressure) equals the ratio (container diameter)/(wall thickness). This motivates the assumption—consistent with abundant empirical data—that the ventricle wall grows thicker as it grows wider. Therefore, cardiac hypertrophy has to multiply sarcomeres also transversally to myofibrils, packing more of them in parallel within each single myocite.

References

1. J. D. Humphrey, *Cardiovascular Solid Mechanics. Cells, Tissues, and Organs* (Springer, New York, 2002).
2. R. S. Chadwick, *Biophysical Journal* **39**, 279 (1982).
3. L. A. Taber, *Annu. Rev. Biomed. Eng.* **3**, 1 (2001).
4. `www.columbiasurgery.org/pat/cardiac/valve.html`.
5. J. H. Omens and Y. C. Fung, *Circ. Res.* **66**, 37 (1990).
6. `www.webschoolsolutions.com/patts/systems/lungs.html`.
7. C. Courneya, `www.cellphys.ubc.ca`.
8. Y. C. Fung, *Biomechanics: Mechanical Properties of Living Tissues*, 2nd edition (Springer, New York, 1993).
9. K. Hayashi, Mechanical properties of soft tissue and arterial walls, in *Biomechanics of Soft Tissues in Cardiovascular Systems*, eds. G. A. Holzapfel and

R. W. Ogden, CISM Courses and Lectures, N. 441 (Springer, Wien, 2003) pp. 15–64.
10. A. Rachev and K. Hayashi, *Annals of Biomedical Engineering* **27**, 459 (1999).
11. J. D. Humphrey and E. Wilson, *J. Biomechanics* **36**, 1595 (2003).
12. A. DiCarlo and S. Quiligotti, *Mech. Res. Comm.* **29**, 449 (2002).
13. A. DiCarlo, Surface and bulk growth unified, in *Mechanics of Material Forces*, eds. P. Steinmann and G. A. Maugin, Advances in Mechanics and Mathematics, Vol. 11 (Springer, New York, 2005) pp. 53–64.
14. A. DiCarlo, S. Naili and S. Quiligotti, *C. R. Mécanique*, **334**, 651 (2006).
15. L. A. Taber, *Appl. Mech. Rev.* **48**, 487 (1995).
16. S. C. Cowin, *Annu. Rev. Biomed. Eng.* **6**, 77 (2004).
17. E. Kröner, *Arch. Rational Mech. Anal.* **4**, 273 (1960).
18. E. H. Lee, *J. Appl. Mechanics* **36**, 1 (1969).
19. E. K. Rodriguez, A. Hoger and A. D. McCulloch, *J. Biomechanics* **27**, 455 (1994).
20. S. Quiligotti, *Theor. Appl. Mech.* **28/29**, 277 (2002).
21. M. Epstein, On material evolution laws, in *Geometry, Continua & Microstructure*, ed. G. A. Maugin, (Hermann, Paris, 1999) pp. 1–9.
22. P. Nardinocchi and L. Teresi, Stress driven remodeling of living tissues, in *Proceedings of the FEMLAB Conference 2005*, (Stockholm, Sweden, 2005).
23. J. D. Humphrey and F. C. P. Yin, *J. Biophysical Society* **52**, 563 (1987).
24. J. D. Humphrey and F. C. P. Yin, *Circ. Res.* **65**, 805 (1989).
25. G. A. Holzapfel, T. Gasser and R. W. Ogden, *J. Elasticity* **61**, 1 (2000).
26. G. A. Holzapfel, T. Gasser and R. W. Ogden, *J. Biomech. Engineering* **126**, 264 (2004).
27. L. A. Taber and D. W. Eggers, *J. Theor. Biol.* **180**, 343 1996.
28. L. A. Taber, *J. Theor. Biol.* **193**, 201 (1998).
29. L. A. Taber, *J. Biomech. Engineering* **120**, 348 (1998).
30. R. Crepaz, W. Pitscheider, G. Radetti and L. Gentili, *Pedriatic Cardiology* **19**, 463 (1998).
31. W. Grossman, *The American Journal of Medicine* **69**, 576 (1980).
32. D. D. Streeter, R. N. Vaishnav, D. J. Patel, H. M. Spotnitz, J. Ross and E. H. Sonnenblick, *Biophysical Journal* **10**, 345 (1970).

Acknowledgements

The work of one or more of the four authors was supported by different funding agencies: the Fifth European Community Framework Programme through the Project HPRN-CT-2002-00284 ("Smart Systems"), GNFM-INdAM (the Italian Group for Mathematical Physics), MIUR (the Italian Ministry of University and Research) through the Project "Mathematical Models for Materials Science" and others, IMA (Institute for Mathematics and its Applications, Minneapolis, MN), Université Paris 12 Val de Marne.